Thin Solid Films 520 (2012) 4068–4073

Contents lists available at SciVerse ScienceDirect

Thin Solid Films

journal homepage: www.elsevier.com/locate/tsf

Study on the antimony tin oxide as a hole injection layer for polymer light emitting diodes

In Sung Song, Soo Won Heo, Ja Ram Ku, Doo Kyung Moon *

Department of Materials Chemistry and Engineering, Konkuk University, 1 Hwayang-dong, Gwangjin-gu, Seoul 143-701, Republic of Korea

ARTICLE INFO

Article history:
Received 7 July 2011
Received in revised form 24 January 2012
Accepted 26 January 2012
Available online 2 February 2012

Keywords:
Antimony tin oxide
Hole injection layer
Polymer light emitting diodes
PEDOT:PSS

ABSTRACT

Poly(3,4-ethylenedioxythiophene):poly(styrenesulfonate) is commonly used as a hole transfer layer in polymer light emitting diodes (PLEDs). However, Indium tin oxide transparent electrodes are corroded by poly(styrenesulfonate) and the erupted indium diffuses into the active layer, which in turn decreases the brightness, efficiency and lifetime of the device. In this study, therefore, antimony tin oxide (ATO) was introduced as a hole injection layer (HIL) in PLEDs. The work function and pH of ATO were −5.1 eV and ~7.5, respectively. When annealed at 200 °C, high conductivity (~0.18 S/cm) was observed, which represents good HIL characteristics. Here, the maximum luminance (26,114 cd/m^2) and maximum efficiency (1.55 cd/A) of the PLEDs were increased by 33% and 20% respectively. Their stability improved as well.

1. Introduction

The fabrication of devices such as organic light emitting devices [1–7], organic thin film transistors [8–11] and polymer solar cells [12–18] as next-generation devices has attracted a great deal of attention. In fact, there have been numerous studies on this topic. The π-conjugated polymers which are used in the active layer of these devices have good stability, good mechanical properties and excellent electro-optical properties. Because they enable the solution process to be used, it is possible to fabricate low-cost and large-area devices by a simple method such as spin coating instead of vacuum deposition. In particular, screen printing [19], ink-jet printing [20–23], micro contact printing [24,25] and the stamping method [26,27] can be applied to polymer light emitting diodes (PLEDs) which use a polymer as an emitting layer, because their solubility is good in organic solvents. As a result, low-cost, large-area, flexible and lightweight devices can be produced.

In the case of PLEDs, electrons and holes are injected from the anode and cathode respectively, recombine in the emitting polymers, fall into the ground state and emit light. To improve the efficiency of PLEDs, the balance of charge injection and transport from each electrode is an important factor [28–32]. For balanced charge injection, multilayer architectures, for example, the introduction of both hole- and electron-transporting layers, is required [33,34]. A number of hole injection/transporting polymers have been reported. Poly (3,4-ethylenedioxythiophene) blended with poly (styrenesulfonate) (PEDOT:PSS) is one of the hole transport layer (HTL) materials, which is extensively used as an interfacial layer to improve the hole transporting properties in most organic devices. Although PEDOT:PSS shows excellent performance, it has some disadvantages, one of which is the formation of an unstable interface between indium tin oxide (ITO) and PEDOT-PSS. Moreover, the PSS in PEDOT:PSS has strongly acidic functional groups which cause the corrosion of ITO and the diffusion of indium into the emitting layer [35].

Recently, hole transporting materials designed to replace PEDOT:PSS have been reported. Niu et al. and Lim et al. introduced thermal cross-linkable hole transporting layers such as thermal curable triphenyldiamine and triphenylamine containing trifluorovinyl ether [36,37]. Using these materials, it was possible to fabricate PLEDs with a multi-layer structure. A wide range of similar hole injection and transporting materials have been developed, but they have the disadvantage of complicated synthesis processes and high production costs. Therefore, in the current study, we fabricated PLEDs by introducing a hole injection layer (HIL).

In this study, we fabricated PLEDs by using antimony tin oxide (ATO), which is neutral and has high conductivity, as the HIL. UV–visible spectroscopy was used to evaluate the transmittance and solvent resistance of the ATO thin film and atomic force microscopy (AFM) was used to observe the surface morphology of the film. Finally, the structure of the fabricated device was optimized by controlling the thickness and thermal treatment temperature of the ATO thin film and thickness of PEDOT:PSS.

2. Materials and measurements

2.1. Materials

Poly [2-methoxy-5-(2-ethylhexyloxy)-1,4-phenylenevinylene] (MEH-PPV) was used for the emitting layer and it was purchased

* Corresponding author. Tel.: +82 2 450 3498; fax: +82 2 444 0765.
E-mail address: dkmoon@konkuk.ac.kr (D.K. Moon).

0040-6090/$ – see front matter © 2012 Elsevier B.V. All rights reserved.
doi:10.1016/j.tsf.2012.01.040

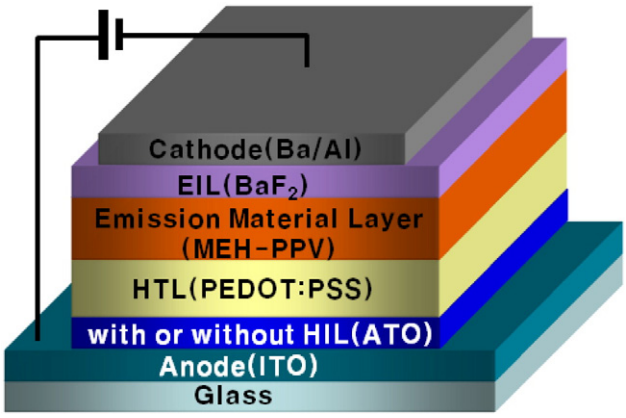

Fig. 1. Structure of PLEDs in this study.

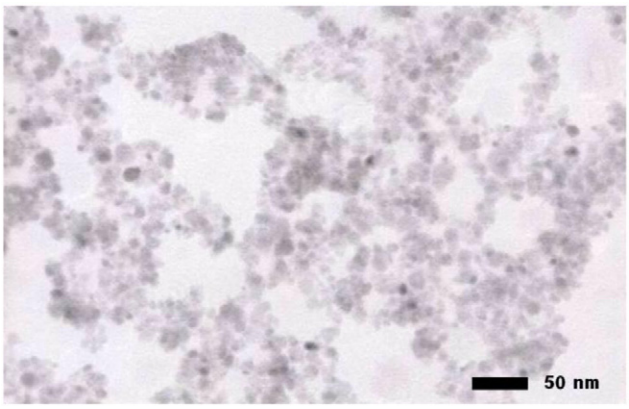

Fig. 3. TEM (operating at 200 kV) image of ATO thin film.

from American Dye Source. The antimony tin oxide solution was purchased from Keeling & Walker and PEDOT:PSS (AI 4083) was purchased from Baytron.

2.2. Measurements

All of the thin films were fabricated using a GMC2 spin coater (Gensys, Korea) and their thickness was measured using an alpha step 500 surface profiler (KLA-Tencor). The absorbance and transmittance of the ATO film were measured using an Agilent 8453 UV–visible spectrometer (HP Agilent) and the conductivity was measured with a 4-point probe station (MST 6000C). Also, the electro-optical properties of the fabricated device were characterized using a Keithley 2400 source meter unit (Keithley) and a PR 670 spectra scan spectroradiometer (Photo Research), while the surface morphology of the thin film was measured using AFM (PSIA XE-150) and transmission electron microscopy (TEM, JEOL JEM-2010).

3. Experiments

3.1. ITO cleaning and film formation of antimony tin oxide

To clean the ITO glass (10 Ω/sq, Samsung Corning), sonication was performed using detergent (Alconox® in deionized (DI) water, 10%), acetone, isopropyl alcohol and DI water, in the order listed, for 20 min each.

The moisture was removed by blowing thoroughly with N_2 gas. In order to ensure the complete removal of all of the remaining water, the ITO was baked on a hot plate for 10 min at 120 °C. For the hydrophilic treatment of the glass surface, it was cleaned for 10 min in a UVO cleaner. To measure the thickness and transmittance of the ATO film spin-coating speed, it was spin-coated at speeds of 1000–4000 rpm and annealed at 200 °C for an hour.

To measure the solvent resistance, the ATO solution which was filtered with a 5 μm polytetrafluoroethylene (PTFE) syringe filter on the cleaned ITO glass was coated at 3000 rpm. Then, it was annealed at 200 °C for an hour to remove the residual solvent. As a result, a 160 nm thick thin film was obtained. The fabricated ATO thin film was rinsed with DI water, chlorobenzene, chloroform and methyl chloride. In addition, the conductivity of the ATO film was measured using a 4-point probe station.

3.2. Fabrication of PLEDs

The PEDOT:PSS and ATO solutions were blended for 24 h after being filtered with a 0.45 μm polyvinylidene fluoride syringe filter and 5 μm PTFE syringe filter, respectively. After dissolving the MEH-PPV, which is applied to the emitting layer in chlorobenzene (0.5 wt.%) and shaking it for 24 h, it was filtered with a 5 μm PTFE syringe filter. To fabricate the PLEDs, ATO solutions were spin-coated (120 nm thick) on the clean patterned ITO glass and annealed at 100 °C–300 °C for an hour. PEDOT:PSS was spin-coated with a range of thicknesses of 30–75 nm and annealed at 120 °C for 20 min. In the case of the orange polymers, they were coated with a thickness of 80 nm and annealed at 90 °C for an hour to remove the residual solvents. The metal electrodes were thermally deposited in a high-vacuum chamber (1.3×10^{-4} Pa or less) in the order of BaF_2 (0.1 Å/s, 2 nm), Ba (0.2 Å/s, 2 nm) and Al (5 Å/s, 200 nm). To protect the organic layer and the electrode layer from H_2O and O_2, a getter was attached to the inside of the glass cover to

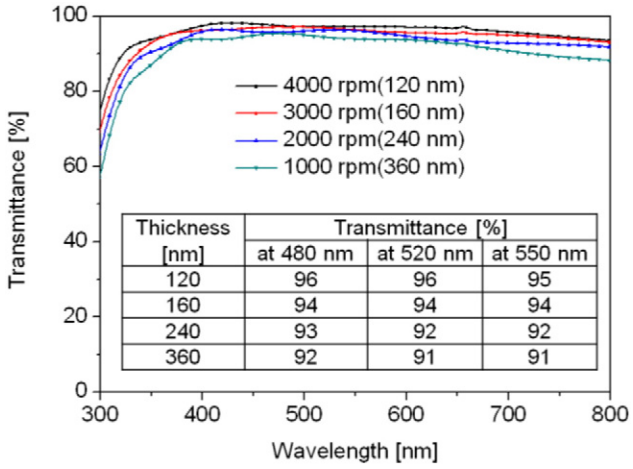

Thickness [nm]	Transmittance [%]		
	at 480 nm	at 520 nm	at 550 nm
120	96	96	95
160	94	94	94
240	93	92	92
360	92	91	91

Fig. 2. Transmittance and thickness of ATO thin films by spin coating speed.

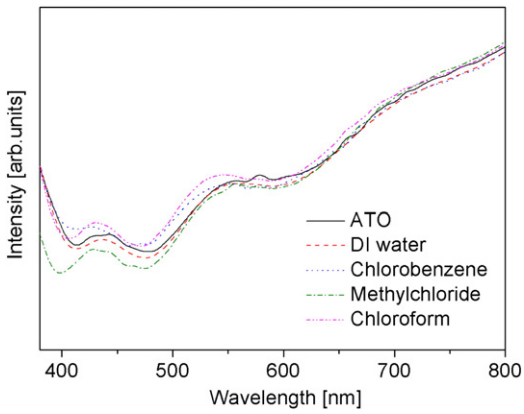

Fig. 4. Absorption spectrums of ATO thin film.

encapsulate the device. The composition of the fabricated device is shown in Fig. 1.

4. Results and discussion

4.1. Thin film of antimony tin oxide

Fig. 2 shows the transmittance as a function of the thickness of the ATO thin film measured by UV–visible spectroscopy. At a thickness of 120 nm, 96% (at 550 nm, visible region) transmittance was observed. In the range of thicknesses from 120 nm to 360 nm, 90% or higher transmittance was detected. In the used ATO solution, SnO_2 and Sb_2O_3 (nano-sized particle metal oxides) are colloidally dispersed in water. The ATO solution was spin-coated on ITO glass followed by thermal treatment at 200 °C. Then, the residual solvent was removed. Consequently producing net-structured channels through which the carriers are able to move. Because of these net-structured channels, the ATO film has high transmittance (Fig. 3). It was expected that the optical absorption and light scattering would be reduced when using the ATO buffer layer as a HIL.

To measure the solvent resistance, the ATO thin film coated on the ITO glass was rinsed with DI water, chlorobenzene, methyl chloride or chloroform. Fig. 4 shows the measured absorbance of the ATO thin films rinsed by the various solvents. According to Fig. 4, almost no change of the absorbance was observed. The SnO_2 and Sb_2O_3 nanoparticles cohered to each other during the thermal annealing process. Therefore, the physical coherence between the ITO and ATO film was improved. As a result, it was found that the ATO thin film showed strong resistance to the solvents. It was expected that surface mixing would not take place when PEDOT:PSS (water base) or the polymer (organic solvent base) was coated on the ATO thin film.

4.2. Characterization of PLEDs

Fig. 1 shows the structure of the PLEDs. In addition, the brightness–voltage and efficiency–current density characteristics of the PLEDs fabricated with various thicknesses (120–360 nm) of the ATO thin film and various annealing temperatures (100–300 °C) are shown in Figs. 5 and 6, respectively. The turn on voltage was 2 V without change of the thickness of ATO and thermal annealing temperature altogether. The best characteristics of the PLEDs were observed when they were annealed at 200 °C.

In addition, to optimize the device structure, the brightness–voltage and efficiency–current density characteristics as a function of the thickness of PEDOT:PSS (HTL) are shown in Fig. 7. The turn on voltage did not vary from 2 V and the best characteristics were observed at a thickness of 40 nm.

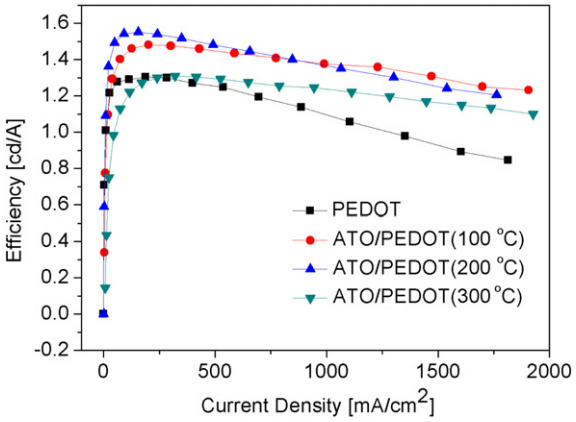

Fig. 6. Efficiency–current density graph by various annealing temperature of ATO thin film (device configuration: ITO/ATO (120–360 nm)/PEDOT:PSS (40 nm)/polymer(80 nm)/BaF_2 (2 nm)/Ba (2 nm)/Al (200 nm)).

Table 1 shows the optimized structure and characteristics of each device. In the case of Device I in which PEDOT:PSS only was used as the HTL, the maximum brightness and maximum efficiency recorded were 19,585 cd/m^2 and 1.30 cd/A, respectively. However, an improvement of the characteristics was observed in Device II and Device III, in which an ATO/PEDOT:PSS structure was fabricated using different annealing temperatures. In particular, in Device III in which the thickness and annealing temperature of the ATO thin film and PEDOT:PSS were optimized, the maximum brightness (26,114 cd/m^2) and maximum efficiency (1.55 cd/A) increased by 33% and 20%, respectively, compared to those of Device I, because ATO facilitated the hole injection from the anode to the PEDOT:PSS layer. The work function of ITO and highest occupied molecular orbital level of PEDOT:PSS were found to be 4.7 eV and 5.2 eV, respectively. The ATO layer (5.1 eV) has the effect of lowering the hole-injection barrier (Fig. 8). In addition, in terms of the conductivity of the ATO film, which were annealed at 100, 200 and 300 °C, values of 0.03, 0.18 and 2.2 S/cm were observed, respectively, which were greater than that of PEDOT:PSS which exhibited values in the range of 10^{-3} to 10^{-4} S/cm. Because of the high conductivity, therefore, it was possible for hole injection to the emission layer to take place quickly. Therefore, the luminance efficiency was enhanced by increasing the probability of recombination with electrons.

To compare the carrier mobility of Device I and Device III, space charge limited current (SCLC) measurements were used. Fig. 9

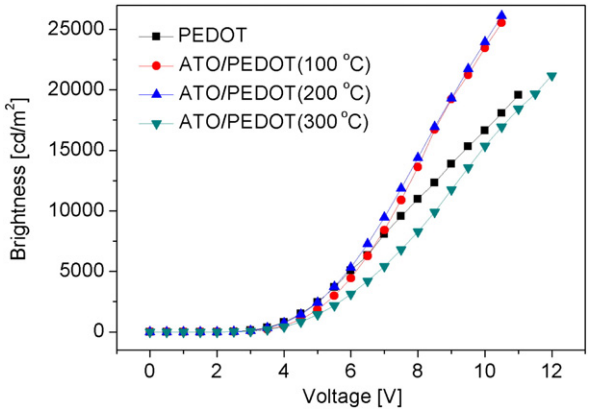

Fig. 5. Brightness–voltage graph by various annealing temperature of ATO thin film (device configuration: ITO/ATO (120–360 nm)/PEDOT:PSS (40 nm)/polymer (80 nm)/BaF_2 (2 nm)/Ba (2 nm)/Al (200 nm)).

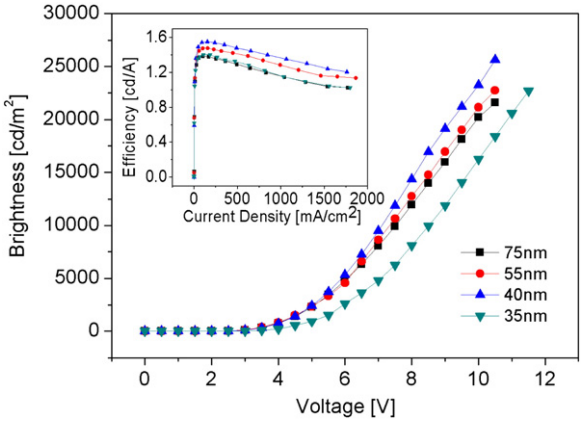

Fig. 7. Brightness–voltage and efficiency–current density graph (inset) by various thickness of PEDOT:PSS (device configuration: ITO/ATO (120 nm)/PEDOT:PSS (35–75 nm)/polymer (80 nm)/BaF_2 (2 nm)/Ba (2 nm)/Al (200 nm)).

Table 1
Characteristics of devices.

Structures		ATO annealing temperature	Turn on voltage [V]	Max brightness [cd/m^2]	Max efficiency [cd/A]	CIE coordinates	λ_{max} [nm]	Full width at half maximum [FWHM, nm]
I	PEDOT:PSS (40 nm)	–	2.0	19,585	1.30	(0.57, 0.42)	586	118
II	ATO (120 nm)/PEDOT:PSS (40 nm)	100 °C	2.0	25,542	1.48	(0.57, 0.42)	584	114
III	ATO (120 nm)/PEDOT:PSS (40 nm)	200 °C	2.0	26,114	1.55	(0.57, 0.42)	584	110
IV	ATO (120 nm)/PEDOT:PSS (40 nm)	300 °C	2.0	21,171	1.30	(0.57, 0.42)	584	118

ITO (170 nm)/I–IV/orange polymer (80 nm)/BaF_2 (2 nm)/Ba (2 nm)/Al (200 nm).

shows the J–V characteristics of a log–log plot and inset shows the J–V curves. SCLC can be described by

$$J = \frac{9}{8}\varepsilon\varepsilon_0\mu\frac{V^2}{L^3} \quad (1)$$

where E is the electric field, ε and ε_0 are the relative dielectric constant and the permittivity of the free space, respectively, and L is the thickness of the organic layer. The hole mobilities of the devices were calculated from Eq. (1) using the J–V curves of the hole-only devices with the configuration ITO/with or without ATO(120 nm)/PEDOT:PSS(40 nm)/MEH-PPV(80 nm)/MoO_3(30 nm)/Al(100 nm). The hole mobility of the hole-only device without ATO layer was calculated to be 4.43×10^{-3} cm^2/V s, whereas the device with ATO layer as the hole injection layer had a value as high as 5.91×10^{-3} cm^2/V s. The hole mobility was 33% higher than that of the device without ATO layer. Because of the high hole mobility of the device with ATO layer, therefore, it was possible for higher maximum brightness and maximum efficiency increased by 33% and 20%, respectively.

Fig. 10 shows the result of accelerated operation-lifetime test of PELDs. In Device I, the extrapolated half-lifetime under the brightness of 10,000 cd/m^2 was 9.3 h. However, half-lifetime of Device III was 14.3 h and 53% was improved, compared to Device I. Two possible reasons may explain this phenomenon. Firstly, the conductivity of HTL was improved by the introduction of the ATO layer, the holes were efficiently injected from ITO to the light-emitting layer. Therefore, because the heat where it is generated in the device was decreased, the lifetime was increased. Secondly, pH of ATO was the neutral with the ~6.5 and was introduced between ITO and PEDOT:PSS layer. The ATO did not erode ITO because of being the neutral. And it prevented the corrosion by PEDOT:PSS.

With increasing annealing temperature, the conductivity of the ATO film increased. However, the characteristics of Device IV were lower than those of Device III, because of the change in the conductivity caused by the increase in the annealing temperature. The sheet resistance of the ATO film which was annealed at 100 °C was very high, viz. 6×10^5 Ω/sq. However, that of the ATO film which was annealed at 300 °C decreased somewhat to 9×10^3 Ω/sq. In our previous study, when the ATO film was annealed at 500 °C, its sheet resistance decreased to 30 Ω/sq, which is sufficiently low for the film to be used as an anode [38]. However, the conductivity of the ATO film (~6500 S/cm) is lower than that of ITO (~8000 S/cm). Therefore, when it was annealed at 300 °C, the ATO film coated on ITO showed the characteristics of an anode, not those of the buffer layer. Because of low conductivity of ATO film, its characteristics are lower than those of Device III.

Fig. 11 shows the EL spectra of the Devices (From I to IV). All of the devices showed the same CIE coordinates (0.57, 0.42). In other words, no color change was observed when ATO was introduced with the HIL. In addition, the color purity of Device III (full width at half maximum (FWHM) of 110 nm) was greater than that of Device I (FWHM of 118 nm).

Fig. 12 shows the surface morphology images of ITO, ITO/ATO, and ITO/ATO/PEDOT:PSS. ITO showed a good morphology with a root

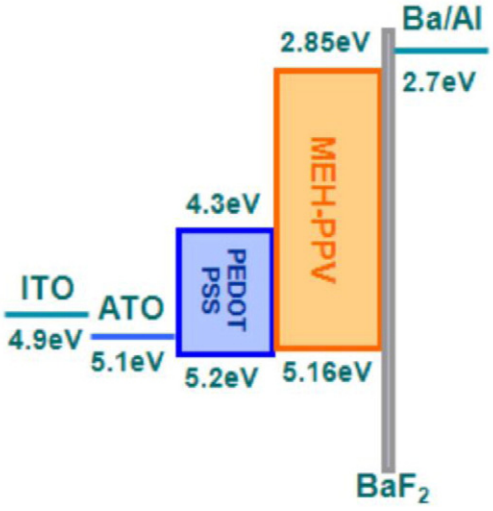

Fig. 8. Energy-band diagram of device.

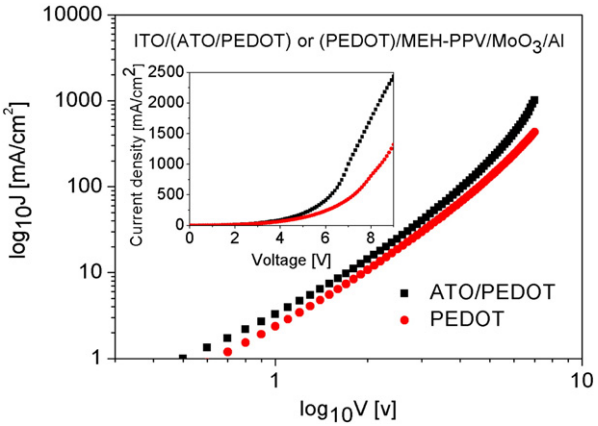

Fig. 9. J–V characteristics of a log–log plot and the J–V curves of hole only devices (inset).

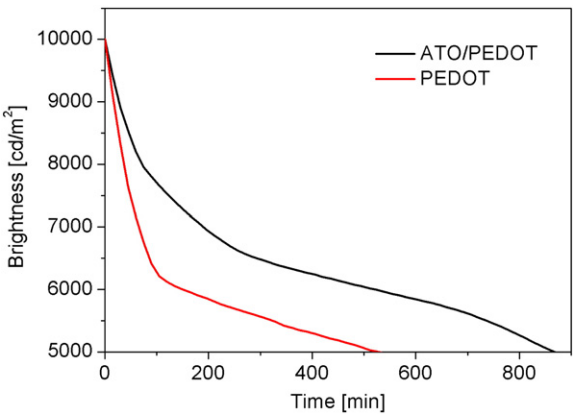

Fig. 10. Accelerated operation-lifetime test of devices.

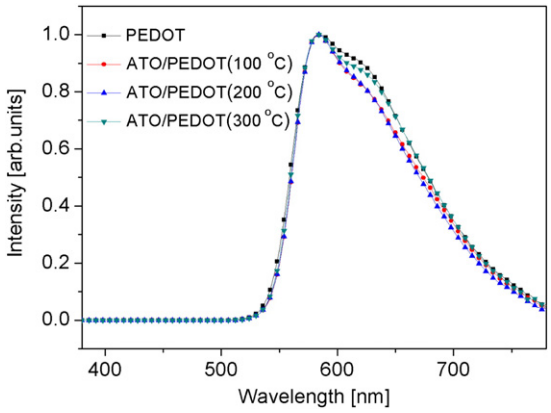

Fig. 11. EL spectrum of devices.

mean square (RMS) of 0.302 nm. When ATO was coated on ITO, on the contrary, the morphology was poorer with an RMS of 7.92 nm. When PEDOT:PSS was coated on ATO, however, the roughness was improved, with an RMS value of 3.36 nm being observed.

5. Conclusion

In this study, the maximum brightness, maximum efficiency and stability of PLEDs were improved by preventing ITO from being corroded by PSS (strong acid) through the development of a HIL/HTL structure (ITO/ATO/PEDOT:PSS) in which ATO was applied as a buffer layer between and ITO and PEDOT:PSS. It was confirmed that ATO is appropriate as an interlayer between the ITO anode and PEDOT:PSS, thanks to its strong solvent resistance properties against DI water and organic solvents such as chlorobenzene, chloroform and methyl chloride. When the ATO thin film was annealed at 200 °C, high

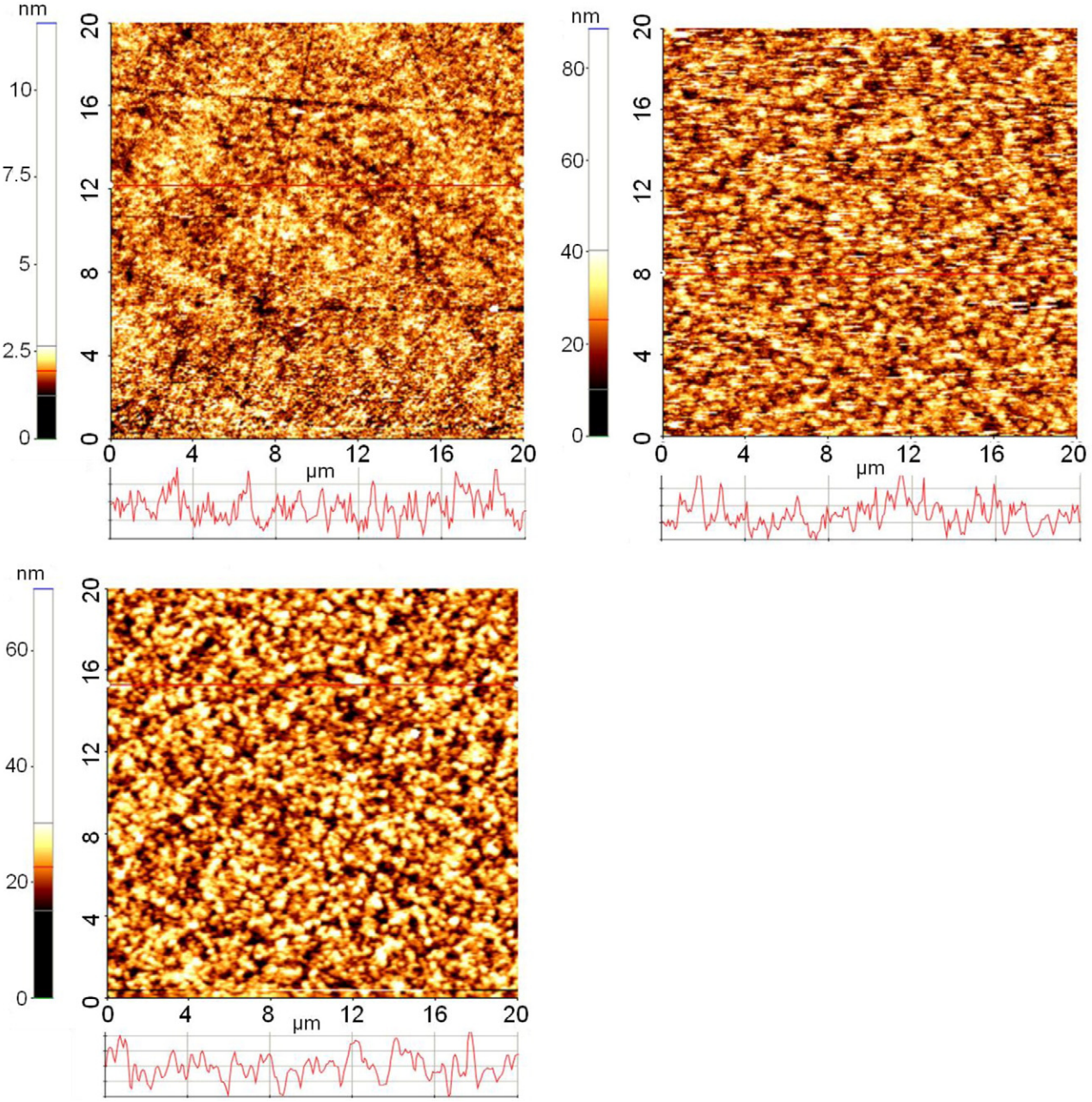

Fig. 12. AFM non-contact mode height images using an aluminum coating on detector side of cantilever. (a) Surface morphology of ITO (RMS: 0.3 nm), (b) Surface morphology of ITO/ATO (RMS: 7.92 nm), (c) Surface morphology of ITO/ATO/PEDOT:PSS (RMS: 3.36 nm).

conductivity (0.18 S/cm) was observed. In addition, the maximum brightness and maximum efficiency were increased by 33% and 20%, respectively, because the hole transfer from the anode to the emitting layer was facilitated. Furthermore, the color purity has improved, with an FWHM value of 110 nm being obtained. It was also confirmed that the device with the ATO thin film was more stable than that in which only PEDOT:PSS was used, because no degradation occurred in it despite the increase in the applied voltage.

Acknowledgments

This work was supported by a grant from the Energy Efficiency and Resources (2008K00203) of the Korea Institute of Energy Technology Evaluation and Planning (KETEP) grant funded by the Korea government Ministry of Knowledge Economy and by Business for Cooperative R&D between Industry, Academy, and Research Institute funded by the Korea Small and Medium Business Administration (00035745-1) in 2009.

References

[1] J.H. Burroughes, D.D.C. Bradley, A.R. Brown, R.N. Marks, K. Mackey, R.H. Friend, P.L. Burns, A.B. Holmes, Nature 347 (1990) 539.
[2] R.H. Friend, R.W. Gymer, A.B. Holmes, J.H. Burroughes, D.D.C. Bradley, D.A.D. Santos, J.L. Bredas, M. Loglund, W.R. Salaneck, Nature 397 (1999) 121.
[3] F. Garten, A. Hilberer, F. Cacialli, E. Esselink, Y.V. Dam, B. Schlatmann, R.H. Friend, T.M. Klapwijk, G. Hadziioannou, Adv. Mater. 9 (1997) 127.
[4] J.Y. Lee, Y.J. Kwon, J.W. Woo, D.K. Moon, J. Ind. Eng. Chem. 14 (2008) 810.
[5] M.J. Park, J.I. Lee, H.Y. Chu, S.H. Kim, T. Zyung, J.H. Eom, H.K. Shim, D.H. Hwang, Synth. Met. 159 (2009) 1393.
[6] K.W. Song, J.Y. Lee, S.W. Heo, D.K. Moon, J. Nanosci. Nanotechnol. 10 (2010) 99.
[7] K.S. Yook, J.Y. Lee, J. Ind. Eng. Chem. 16 (2010) 181.
[8] Z. Bao, J.A. Rogers, H.E. Katz, J. Mater. Chem. 9 (1999) 1895.
[9] G. Horowitz, Adv. Mater. 10 (1998) 365.
[10] L.L. Chua, J. Zaumseil, J.F. Chang, E.C.W. Ou, P.K.H. Ho, H. Sirringhaus, R.H. Friend, Nature 434 (2005) 194.
[11] X. Huang, C. Zhu, S. Zhang, W. Li, Y. Guo, X. Zhan, Y. Liu, Z. Bo, Macromolecules 41 (2008) 6895.
[12] S.W. Heo, J.Y. Lee, H.J. Song, J.R. Ku, D.K. Moon, Sol. Energy Mater. Sol. Cells 95 (2011) 3041.
[13] S.W. Heo, K.W. Song, M.H. Choi, T.H. Sung, D.K. Moon, Sol. Energy Mater. Sol. Cells 95 (2011) 3564.
[14] J.Y. Lee, W.S. Shin, J.R. Haw, D.K. Moon, J. Mater. Chem. 19 (2009) 4938.
[15] J.Y. Lee, S.W. Heo, H. Choi, Y.J. Kwon, J.R. Haw, D.K. Moon, Sol. Energy Mater. Sol. Cells 93 (2009) 1932.
[16] Y.J. Cheng, S.H. Yang, C.S. Hsu, Chem. Rev. 109 (2009) 5868.
[17] G. Dennler, M.C. Scharber, C.J. Brabec, Adv. Mater. 21 (2009) 1323.
[18] M. Skompska, Synth. Met. 160 (2010) 1.
[19] Z. Bao, Y. Feng, A. Dodabalapur, V.R. Raju, A. Lovinger, Chem. Mater. 9 (1997) 1299.
[20] J. Bharathan, Y. Yang, Appl. Phys. Lett. 72 (1998) 2660.
[21] S.C. Chang, J. Bharathan, Y. Yang, Appl. Phys. Lett. 73 (1998) 2561.
[22] T.R. Hebner, C.C. Wu, D. Marcy, M.H. Lu, J.C. Sturm, Appl. Phys. Lett. 72 (1998) 519.
[23] T. Aernouts, T. Aleksandrov, C. Girotto, J. Genoe, J. Poortmans, Appl. Phys. Lett. 92 (2008) 03306.
[24] J.A. Rogers, Z. Bao, L. Dhar, Appl. Phys. Lett. 73 (1998) 294.
[25] M. Nishizawa, K. Takoh, T. Matsue, Langmuir 18 (2002) 3645.
[26] J.H. Huang, Z.Y. Ho, T.H. Kuo, D. Kekuda, C.W. Chu, K.C. Ho, J. Mater. Chem. 19 (2009) 4077.
[27] D.H. Wang, D.G. Choi, K.J. Lee, O.O. Park, J.H. Park, Org. Electron. 11 (2010) 599.
[28] D. Liu, F. Teng, Z. Xu, S. Yang, L. Qian, Q. He, Y. Wang, X. Xu, J. Lumin. 122 (2007) 656.
[29] K.R. Choudhury, J. Lee, N. Chopra, A. Gupta, X. Jiang, F. Amy, F. So, Adv. Funct. Mater. 19 (2009) 491.
[30] S.R. Tseng, Y.S. Chen, H.F. Meng, H.C. Lai, C.H. Yeh, S.F. Horng, H.H. Liao, C.S. Hsu, Synth. Met. 159 (2009) 137.
[31] D. Madhwal, S.S. Rait, A. Verma, A. Kumar, P.K. Bhatnagar, P.C. Mathur, M. Onoda, J. Lumin. 130 (2010) 331.
[32] D. Song, S. Zhao, F. Zhang, Z. Xu, J. Li, X. Yue, H. Zhu, L. Lu, Y. Wang, J. Lumin. 129 (2009) 1978.
[33] J. Lee, B.J. Jung, J.I. Lee, H.K. Shim, J. Mater. Chem. 12 (2002) 3494.
[34] S.H. Oh, D. Vak, S.I. Na, T.W. Lee, D.Y. Kim, Adv. Mater. 20 (2008) 1624.
[35] M.P. de Jong, L.J. van Ijzendoorn, M.J.A. de Voigt, Appl. Phys. Lett. 77 (2000) 2255.
[36] Y.H. Niu, Y.L. Tung, Y. Chi, Chem. Mater. 17 (2005) 3532.
[37] B. Lim, J.T. Hwang, J.Y. Kim, J. Ghim, D. Vak, Y.Y. Noh, S.H. Lee, K. Lee, A.J. Heeger, D.Y. Kim, Org. Lett. 8 (2006) 4703.
[38] I.S. Somg, D.J. Ma, S.W. Heo, D.K. Moon, SID Symposium Digest of Technical Papers, 40, 2009, p. 1306.